

RESEARCH / INVESTIGACIÓN

Conjugation strategies on functionalized iron oxide nanoparticles as a malaria vaccine delivery system

Aswan Al-Abboodi¹, Hussain A. Mhouse Alsaady¹, Shaima R. Banoon¹, Mohammed Al-Saady² DOI. 10.21931/RB/2021.06.03.20

Abstract: Vaccination has been used effectively to protect from infectious diseases and non-infectious diseases such as cancer and allergies. Different forms of particulate arrangements, including nanoparticles, virus-like particles (VLPs), and virosomes, have been built recently depending on the type of pathogen to be targeted. The ability to conjugate the recombinant *Plasmodium yoelii*, 19-kDa C-terminal fragment of merozoite surface protein 1 (PyMSP1₁₉) on the surface of superparamagnetic magnetite nanoparticles (SPIONs) was explored as a new technique of enhancing vaccination against malaria. Different conjugation strategies were performed to correlate the effects of nanoparticle chemistry surfaces to bind later with the malaria protein. (SPIONs) were prepared by chemical coprecipitation method and coated with 3-aminopropyltriethoxysilane (APTS) alone (as a surface coater), or with both APTS and polyethylene glycol (PEG) (as a shield to protect the malaria protein from proteolytic enzymes) by using a modified silanisation method.

X-ray powder diffraction (XRD, Philips Model) patterns indicated that the SPIONs were of high purity with an inverse spinel structure. Fourier Transform Infrared Spectroscopy (FTIR) was collected using PerkinElmer Spectrum 100 Series; spectra of uncoated and coated magnetite nanoparticles confirmed that the silane layer had been coated on the surface Fe₃O₄. The SPIONs were superparamagnetic as investigated by Vibrating Sample Magnetometry (VSM, Princeton Applied Research, model ISS) and relatively stable in aqueous phase at room temperature and could also be quickly recovered from suspension using an external magnet. Introduce the carboxyl groups onto the SPIONs surfaces, resulting in a relatively high protein binding capacity onto the nanoparticle surfaces.

The bare particles had a mean size of around 20 nm with a relatively narrow size distribution. 82% of African Green Monkey fibroblast (COS-7) were alive in nanoparticle suspension using the MTT assay method. The quantity of protein explicitly bound to particles was determined using Sodium Dodecyl Sulfate (SDS) - Polyacrylamide Gel Electrophoresis (PAGE). SDS-PAGE. When the conjugation blend was prepared in EDC, there was approximately 100% binding between PyMSP1₁₉ and the Fe₃O₄-COOH particles because no protein band was apparent at the expected molecular weight for PyMSP1₁₉ (45 kDa).

The current study investigates the theory that the gradual, persistent release of the malaria antigen may stimulate and maintain an elevated level of immune response for an extended period *in vivo*, which will be the scope of future work.

Key words: Malaria vaccine, Superparamagnetic nanoparticles, protein functionalization.

Introduction

Iron oxide nanoparticles such as magnetite Fe₃O₄ or maghemite γ-Fe₂O₃ are promising materials for applications in biomedicine and bioengineering areas^{1-3,30} These nanoparticles have attracted great interest due to their unique properties^{4,31} such as narrow size distribution, biocompatibility, non-toxicity, and ability to be detected and manipulated with an external magnetic field. Both are generally appropriate and safe for *in vivo* biomedical applications⁴. However, the utilization of these nanoparticles is still subject to many limitations, including surfaces containing hydroxyl groups that cannot bond covalently with biomolecules. Therefore, examining the best method to conjugate high protein binding capacity is an urgent issue because the most excellent technique for increasing vaccine efficiency still needs investigation since many diseases are still without effective vaccines, such as malaria disease.

The Coprecipitation technique is the most common method to prepare iron oxide nanoparticles. Both sodium hydroxide (NaOH) and ammonium hydroxide (NH₄OH) have been used to detect whether the basicity manipulates the crystallization process during particle formation^{8,32}. Various surface modification techniques have been used to enhance nanoparticles' diagnosis and therapeutics potential in biomedicine applications⁵. Successful conjugation of biomolecules to the surface of magnetic particles is critical to their applicability⁵. Therefo-

re, a versatile method of surface functionalization of SPIONs is often required, which sensitively balances the intermolecular forces concerning biomolecules such as proteins and antibodies attached to the particles' outer layer. However, conjugation of a desired functional group at the right orientation on the nanoparticle surface remains a significant challenge^{7,33,44}. The method of surface modification of iron oxide by using organosilane reagent [amino-silane reagent (3-aminopropyltriethoxysilane, APTS)] is relatively robust, with many parameters such as silane concentration, temperature, time, and solvent type that can be optimized to create diffused functionalized magnetic particles for consequent tagging with biomolecules⁵.

Some vaccines are still challenged and need effective strategies to obtain good control for malaria vaccines. Protein vaccine is one strategy that can generate both humoral and cellular immune responses, primarily when it supports by promoter injections^{12,34}. Magnetofection is a suitable device for protein delivery, gene therapy, and gene expression^{14,42,43}; therefore, magnetic nanoparticles have been chosen for this study to prove its achievability as a proposed protein delivery carrier of malaria vaccine to use it later as a vaccine carrier for other some parasitic diseases that their vaccines are underdeveloped until now. Substantial development in the malaria vaccine field has been presented in the current study; the key to this

¹ Department of Biology, College of Science, University of Misan, Misan, Iraq.

² Department of Mechanical and Aerospace Engineering, Monash University, Clayton, Australia.

success is iron oxide nanoparticles' use to deliver malaria protein (antigen) in an effectual technique to where it matters.

Materials

Analytical grade reagents for magnetite nanoparticles synthesis included Fe (III) chloride hexahydrate ($\text{FeCl}_3 \cdot 6\text{H}_2\text{O}$ >99%) from Ajax Finechem (NSW Australia), Fe (II) sulfate ($\text{FeCl}_2 \cdot 7\text{H}_2\text{O}$ >99%) from Ajax Chemical (Sydney, Australia), sodium hydroxide (NaOH), and trisodium citrate dihydrate ($\text{C}_6\text{H}_5\text{Na}_3\text{O}_7 \cdot 2\text{H}_2\text{O}$) from Sigma Aldrich (Sydney, Australia). All materials including 3-aminopropyltriethoxysilane (APTS, 95%), Polyethyleneglycol (PEG), absolute ethanol ($\text{C}_2\text{H}_5\text{OH}$, 99.5%) glutaraldehyde (10%), succinic anhydride, phosphate buffered saline (PBS, 0.01M, pH 7.4), and the conjugating agents N-hydroxysulfosuccinimide (NHS), 1-ethyl-3-(3-dimethylaminopropyl) carbodiimide (EDC), N, N-dimethylformamide (DMF) were supplied by Sigma Aldrich (Sydney, Australia). African green monkey kidney cells (COS-7 cell lines) were kindly provided by staff at Prof. Ross Coppel's laboratory (Department of Microbiology, Monash University, Australia). Dimethylsulfoxide (DMSO), 3-(4,5-87-90% dimethyl-2-thiazol-2-yl-2, 5-diphenyltetra-zolium bromide (MTT), penicillin/ streptomycin, foetal calf serum and other related reagent grade chemicals were acquired from Invitrogen (Carlsbad, California, USA) and used to measure the toxicity of the as-synthesised nanoparticles.

Methods

Synthesis and coating of Magnetite nanoparticles

Magnetite nanoparticles were prepared using the procedure reported in (8), in which a chemical coprecipitation method was used with some modification. Trisodium citrate was used as an electrostatic stabilizer to create an electrostatic double layer and reduced the extent of agglomeration^{12,13,41}. In a typical experiment, ferric chloride (0.005 mol) and ferrous chloride (0.0025 mol) (molar ratio 2:1) were dissolved in deionized water (50 ml). To raise the pH value, sodium hydroxide solution (20 ml, 1.5 M, including 0.005 mol trisodium citrate) was added to a 100 ml three-necked flask. The precipitation was done by drop-by-drop addition of iron salts solution to the mixture of NaOH and trisodium citrate under vigorous stirring (homogenization string rate was 1500 rpm) for 1h at 80 °C in a nitrogen (N_2) atmosphere. The color of the bulk solution immediately turned from orange to black. The nanoparticles were then split from the solution by a permanent magnet and cleaned several times with ethanol and distilled water before re-suspended in water.

APTS is an amino-functional silane-coupling agent used to immobilize physiologically active molecules. The hydroxyl groups on the magnetite surface can be easily coupled with silanes by forming covalent bonds through condensation reaction to give a siloxane linkage, as Scheme 1 shows. In this work, ethanol was used to change the medium from water. 0.43g of Fe_3O_4 nanoparticles were dispersed in 9.7ml ethanol by sonication for 10 min. 0.3ml of 3-aminopropyltriethoxysilane (APTS) was added, and the resulting solution was transferred into a round-bottomed flask to carry out the silanisation reaction at 25 °C under N_2 atmosphere overnight in a Schlenk system. The Fe_3O_4 - APTS magnetic nanoparticles were recovered from the reaction mixture using a permanent magnet. The supernatant was removed, and the precipitates were washed several times

with ethanol and then with water. The high molecular weight of PEG polymer was mixed with silane to possibly improve the biocompatibility and dispersibility of Fe_3O_4 nanoparticles^{15,16}.

SPIONs Characterisations

Powder X-Ray diffraction (XRD)

X-ray powder diffraction (XRD) measurements were used to identify the crystalline phase of the particles before and after coating. XRD was performed on a Philips PW 1140/90 diffractometer using monochromatized x-ray beams from $\text{CuK}\alpha$, $\lambda = 1.54 \text{ \AA}$ radiation at a scan rate of 1° min^{-1} from 5° to 60° with a step size of 0.02° . The scanning voltage was 50KV, and the scanning current was 20 mA.

Vibrating Sample Magnetometry (VSM)

The particular values for the inundation magnetization measurements were directly acquired on a predetermined weight of SPIONs before and after coating using Vibrating Sample Magnetometry (VSM, Princeton Applied Research, model ISS) working at room temperature. A recognized weight of the samples was placed into the VSM sample holder. A top magnetic field of approximately 15K0e was used. The saturation magnetization values were standardized to the mass of samples to yield specific magnetization, M_s (emu g^{-1}).

Fourier Transform Infrared Spectroscopy (FTIR)

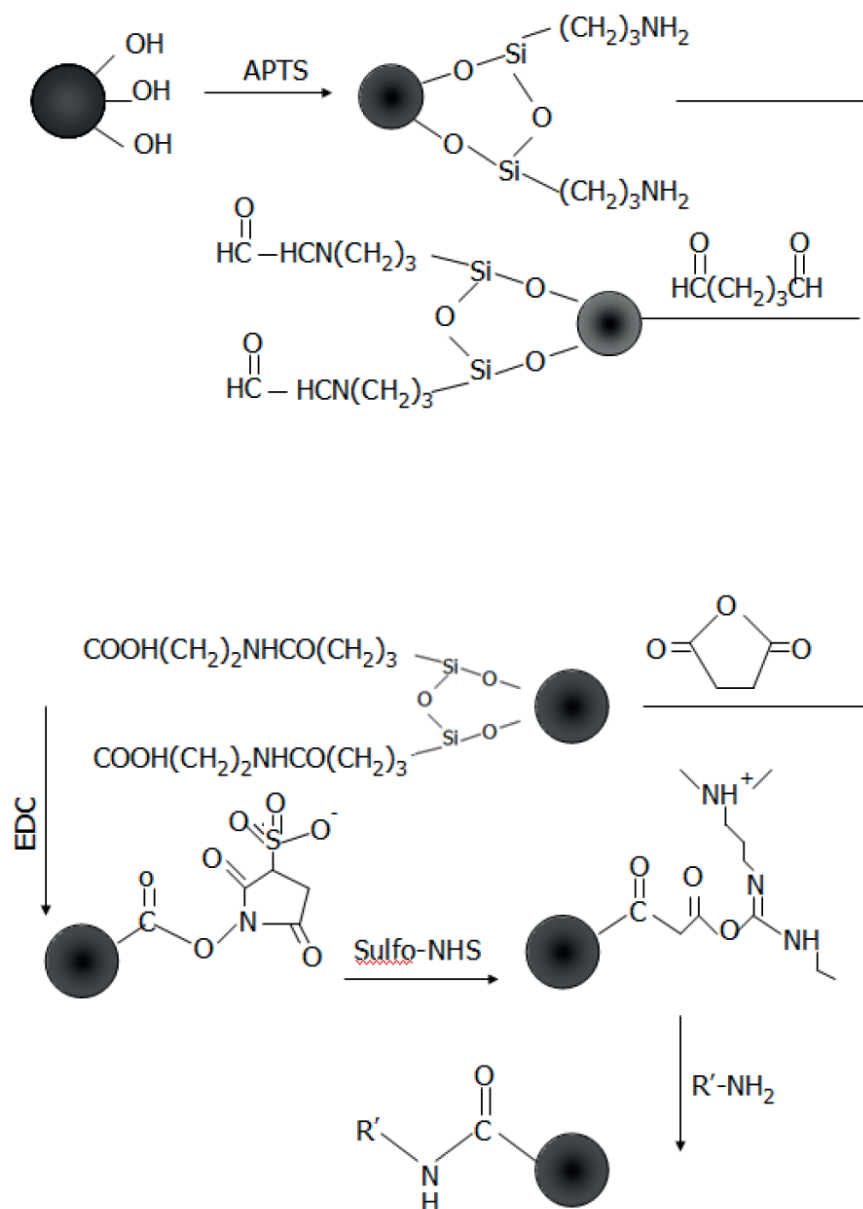
FTIR spectra of the nanoparticles were collected on an FTIR spectrophotometer using PerkinElmer Spectrum 100 Series FT-IR spectrometer in a wave number varying from 4000 to 400 cm^{-1} with a resolution accuracy of 4 cm^{-1} under ambient conditions. Before compacting, all samples were dried at 70°C for 48h. A small amount of each sample dry powder was thoroughly mixed and crushed with dried KBr using a mortar and pestle. The mixture was pressed into pellets using 8 tons/ cm^2 of pressure for 2 minutes to form discs for analysis.

Transmission Electron Microscope (TEM)

TEM was used to determine the size and morphology of the nanoparticles. The nanoparticle suspension was diluted, and a few drops were put on a carbon-stabilized grid (200 meshes). The grids were left in the oven at 50°C overnight. Sample grids were attached to the sample holder on a Hitachi H7500 TEM instrument at an accelerating voltage of 120 kV microscope. The mean diameter of the size distribution was determined by measuring more than 150 particles from TEM images using *Image J*⁹.

MTT assay

To evaluate whether the particles could be used for biomedical applications, a non-radioactive colorimetric MTT assay¹⁰ was performed to measure the cell cytotoxicity. African Green Monkey Fibroblast (COS-7) cells were seeded on a 96-well microtiter plate at a concentration of 2×10^4 /well and cultured in a complete RPMI (C-RPMI) medium supplemented with 10% fetal calf serum (FCS). The plate was incubated at 37°C and 5% CO_2 overnight. Three different concentrations of bare and coated nanoparticles (0.1 mg/ml, 1 mg/ml and 10 mg/ml) were added for a further 24h incubation. The control well group was a culture medium with no particles. All samples and the control were tested in triplicate, with the results conveyed as mean \pm standard deviation shown as error bars in the MTT plots. 5 μl of a solution of 5mg/ml MTT (3-(4,5-dimethylthiazol-2-yl-2, 5-diphenyltetra-zolium bromide) dissol-



Scheme 1. Silane chemistry approaches to functionalize Fe_3O_4 particles with $-\text{NH}_2$, $-\text{CHO}$, and $-\text{COOH}$.

2011

ved in PBS pH 7.4 was added to each well and incubated for 4h at 37°C in the 5% CO_2 incubator. After incubation for 4h, the medium was removed from the plate and rinsed with PBS. MTT is a yellow-colored, water-soluble, and tetrazolium salt. Living cells can metabolize this salt in their mitochondria by active mitochondrial reductase enzyme into a water-insoluble and dark blue ring, Formazan derivative. Dead cells can now reduce tetrazolium salt; thus, the conversion can be related to the amount of Formazan crystals formed. Subsequently, ring Formazan crystals can be dispersed in an organic solvent such as dimethyl sulfur oxide (DMSO). Therefore, 100 μl of 5mg/ml of (DMSO) was added to each well in the plate to dissolve the crystals, and the plate was incubated for 1h. The absorbance of each well was read on a microplate reader (Magellan, Tecan, Australia) at wavelengths of 570nm and 690nm. The net absorbance was calculated by $(A_{570} - A_{690})$ (A refers to the area means absorbance). The relative cell viability (%) was calculated as $([A_{\text{sample}}] / [A_{\text{control}}]) * 100\%$, with the resultant value representing the number of living cells.

Surface functionalization of Fe_3O_4 - APTS nanoparticles

The particles were modified to introduce aldehyde or car-

boxylic functional groups. 20 ml of 10% glutaraldehyde was added to the precipitate of silane-coated magnetic particles (Fe_3O_4 - APTS) prepared previously, and the reaction mixture was left under gentle agitation for 3hrs at room temperature (25°C) to introduce aldehyde functional groups. After 3hrs, the Fe_3O_4 - CHO particles were steadied with a magnet and then cleaned several times with PBS via magnetic parting and then re-dispersed. To create the carboxyl functional groups, succinic anhydride was added to the Fe_3O_4 - APTS nanoparticles (1:20 wt/ wt) suspended in DMF. The mixture was agitated for 3hrs under an N_2 atmosphere. Subsequently, the Fe_3O_4 - COOH derivatized particles were washed two times with DMF followed by PBS. The washed particles were suspended in PBS and stored at 4°C for further use.

Results

Characterization of nanoparticles

X-ray powder diffraction (XRD) was performed to characterize the crystal phase of as-synthesized nanoparticles

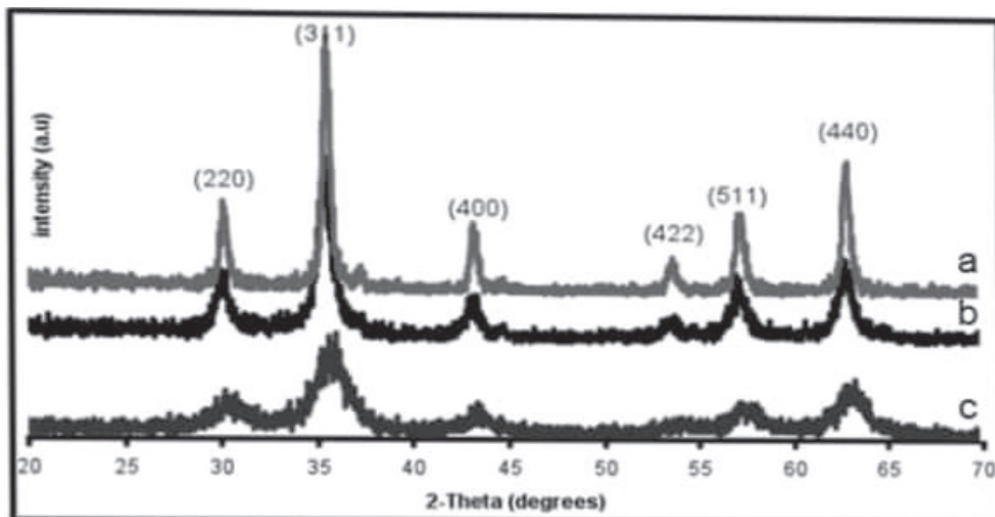


Figure 1. Indexed X-ray diffractograms of (a) Fe_3O_4 , (b) Fe_3O_4 - APTS, and (c) Fe_3O_4 - APTS+PEG nanoparticles.

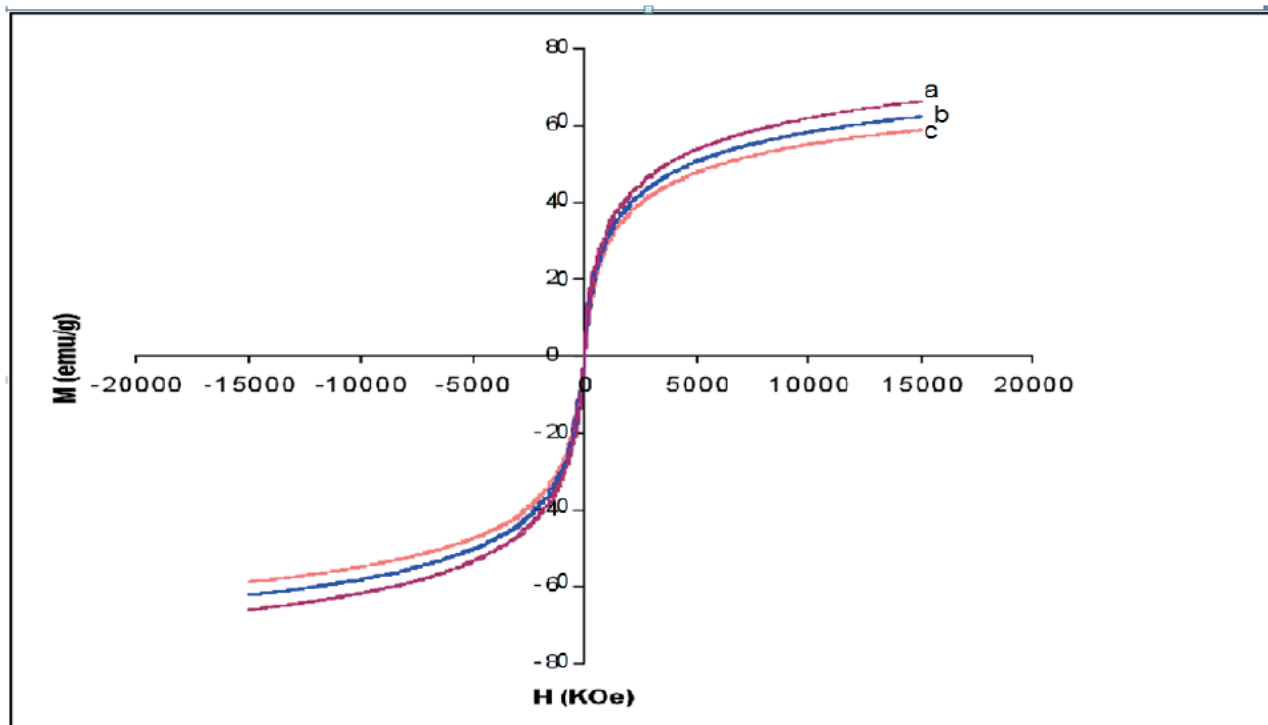


Figure 2. Magnetization curves of (a) Fe_3O_4 , (b) Fe_3O_4 - APTS and (c) Fe_3O_4 - APTS+PEG nanoparticles. (H) Applied magnetic field (kOe); (M) Magnetization (emu/g).

(Fig. 1). The different peaks of Fe_3O_4 marked by their indices: (220), (311), (400), (422), (511), and (440) at 2θ can be referred to as the cubic structure of Fe_3O_4 . Magnetic features of the as-synthesized nanoparticles were investigated by VSM measurement at room temperature (Fig. 2). The bare Fe_3O_4 displayed relatively high magnetization (67 emu/g) at 15kOe. The magnetization of silane-coated Fe_3O_4 - APTS nanoparticles was calculated to be 63.3 emu/g (Fig. 2b), slightly diminished in comparison to bare Fe_3O_4 due to the non-magnetic silane layer. In addition, Fe_3O_4 - APTS+PEG nanoparticles have a magnetization of 58.9 emu/g, due to the thickness of the silane and PEG coating.

TEM images of bare and silane-coated nanoparticles were taken to investigate the particles' size, shape, and uniformity. The bare particles had a mean size of around 20 nm with a relatively good size distribution (Fig. 3a). Scanning electron micrograph images for magnetic nanoparticles before and af-

ter silanisation are shown in Fig. 3, confirming the size of bare Fe_3O_4 of around 20nm. FTIR spectra of uncoated and coated magnetite nanoparticles are shown in Fig. 4. The wide band of $3600 - 3300 \text{ cm}^{-1}$ paralleled the O-H stretching tremor of a trace amount of water due to physisorbed water and surface hydroxyls. After silanisation, the characteristic bands of Si-O-C at 1086 and 1155 cm^{-1} appeared (Fig. 4b), confirming that silane layer had been coated on the surface of Fe_3O_4 .

In vitro cytotoxicity evaluation

To investigate the percentage of cell viability due to the introduction to nanoparticles, the viabilities of African Green Monkey fibroblast (COS-7) cells in models with both bare and coated magnetite were studied by the MTT assay method to evaluate whether these nanoparticles are suitable for biomedical applications. This method measures the mitochondrial dehydrogenase activity of viable cells, with materials inducing

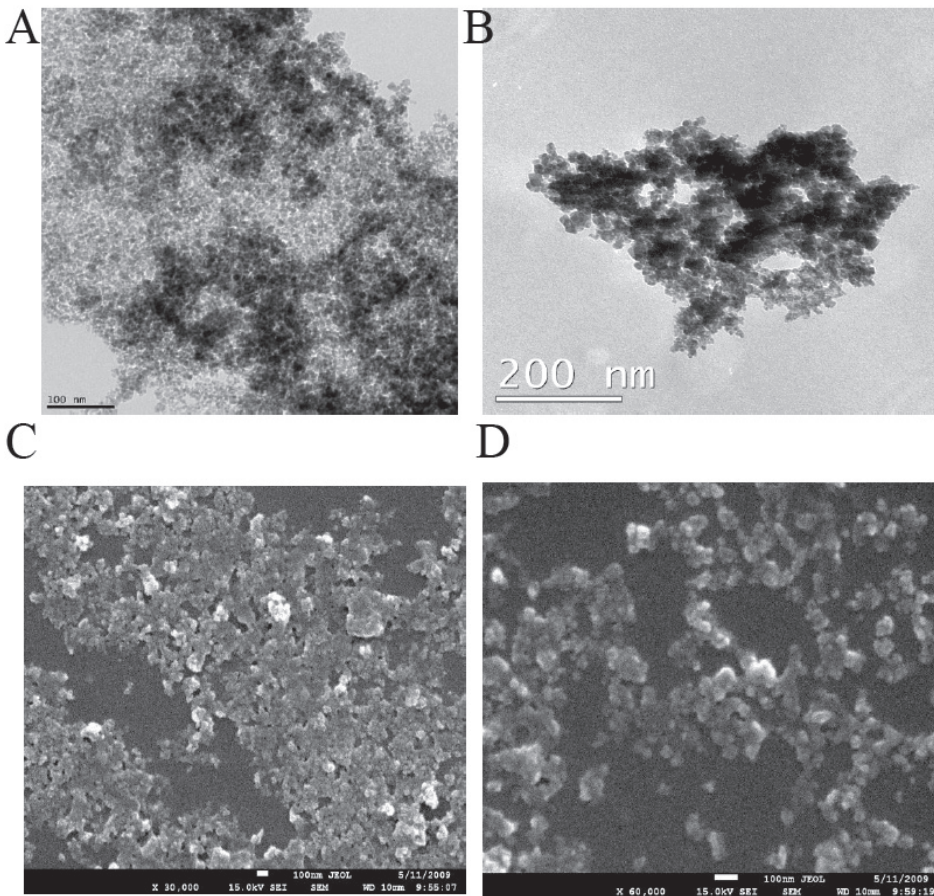


Figure 3. TEM images showing the morphology of (a) Fe_3O_4 ; (b) Fe_3O_4 – APTS, SEM images of (c) Fe_3O_4 ; (d) Fe_3O_4 – APTS.

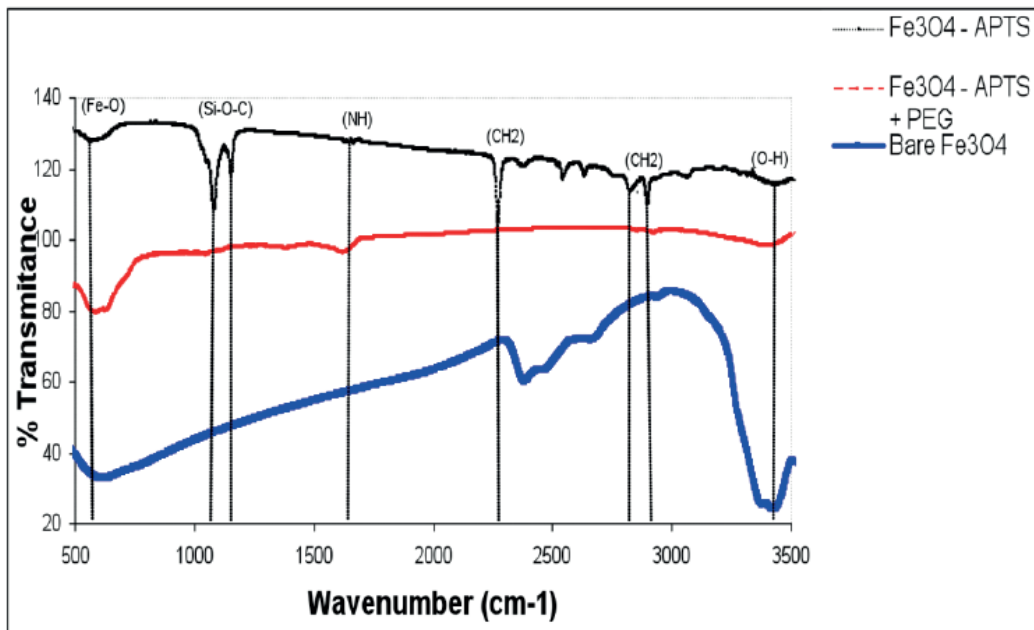


Figure 4. FTIR spectra of Fe_3O_4 , Fe_3O_4 – APTS, and Fe_3O_4 – APTS+PEG.

cell viability of more than 80%, often recognized as biocompatible²². All the nanoparticles samples (three different concentrations for each sample) from a 24 h incubation led to a decrease in the viability of COS-7 cell lines compared to the control. As shown in Fig. 5, when the cells were incubated with 0.1 mg/ml bare Fe_3O_4 solution, more than 82% of cells remained alive, whereas the cell viability decreased to 34% and 12.5% with increasing concentrations to 1 mg/ml and 10 mg/ml, respectively.

Surface functionalization of Fe_3O_4 – APTS nanoparticles

The introduction of $-\text{COOH}$ and $-\text{CHO}$ groups on the magnetite surface was confirmed with FTIR spectroscopy (Fig. 6). The spectrum of the functionalized SPIONs with $-\text{COOH}$ showed the characteristic absorption peak at 1634 cm^{-1} corresponding to the symmetric COO^- stretching. The characteristic absorption peak $-\text{C-O-C}-$ at 2993.4 cm^{-1} was observed in the spectrum of the $-\text{COOH}$ group activated on the silane-coated Fe_3O_4 nanoparticles.

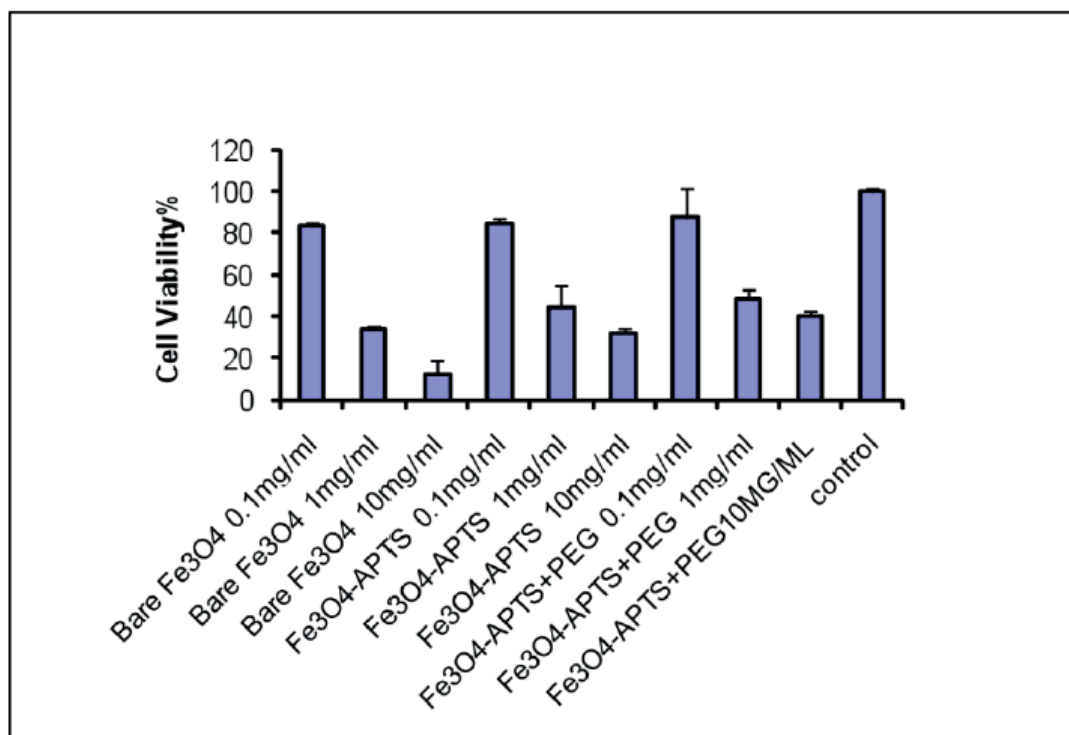


Figure 5. MTT assay of Fe₃O₄, Fe₃O₄ – APTS, and Fe₃O₄ – APTS+PEG.

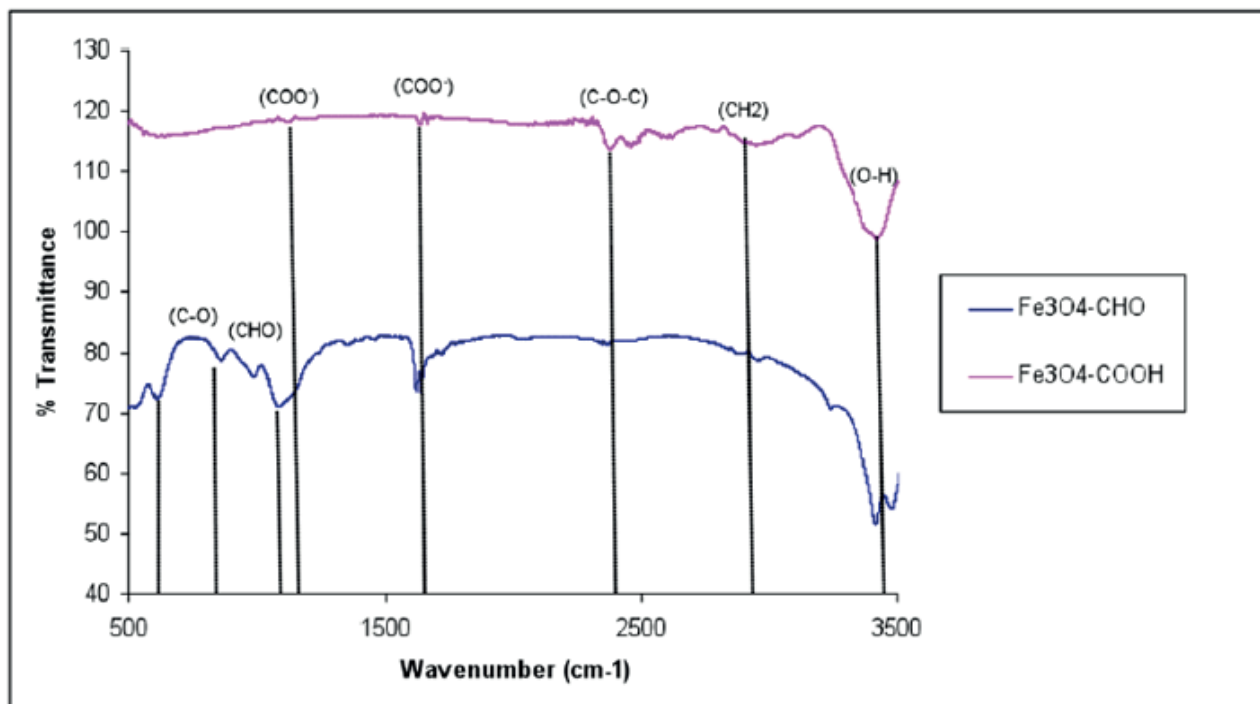


Figure 6. FTIR spectra of functionalized Fe₃O₄ – COOH and Fe₃O₄ – CHO nanoparticles.

DISCUSSION

Characterization of nanoparticles

The X-ray diffraction results showed in (Fig. 1) are in good agreement with the theoretical values (JCPDS 19-629) of the standard XRD reference pattern of pure magnetite. A clean Fe₃O₄ cubic spinel phase can be confirmed. Generally, there was no significant shift in the highest position due to the

presence of amino silane. The broader peak that appeared at about 23.4° in the coated particles Fe₃O₄ – APTS+PEG attributed to the existence of an amorphous layer possibly due to the presence of polymer. The magnetic properties presented in (Fig. 2), in all cases, the magnetization plots exhibited zero remanence and coercivity with no hysteresis loop, indicating that these nanoparticles were superparamagnetic^{17,18,35}, due to their sizes rendering single magnetic domains¹⁹. The TEM images illustrated in (Fig 3) revealed a thin silane layer favorable

to keep the high magnetization and stability, while it was also convenient for modification on the nanoparticles surface²⁹. In the three presented samples in (Fig. 4), the presence of Fe₃O₄ core could be seen by the strong absorption band 579 cm⁻¹, corresponding to the Fe-O bond of Fe₃O₄^{20,21,36}. The strong C-O-C, CH₂, and -CH peaks indicated that PEG was bonded to the surface through a reaction of PEG-silane with -OH group on the nanoparticle's surface¹¹.

In vitro cytotoxicity evaluation

Fig. 5 showed the results of the MTT assay. This result proved the biocompatibility of the synthesized magnetite nanoparticles at minimal concentrations (<0.1 mg/ml), comparable to the standard dosage for particulate vaccine typically measured in micrograms²³. The toxicity of SPIONs may correlate to the capability of these nanoparticles to damage DNA via magnetite oxidation. Karlsson *et al.*²⁴ indicated that magnetite nanoparticles could cause a minimal amount of toxicity (examined with a comet assay) due to the effectiveness in causing oxidative DNA lesions in cultured A549 cells (the human lung epithelial cell line). A small adverse effect on cell viability at low concentrations suggested that citrate groups on the surface of Fe₃O₄ play an essential role in providing some protection against cell toxicity and reducing the toxic effect of magnetic solution^{25,26,37}. The coated SPIONs with silane alone and silane with PEG showed slightly reduced toxic effects at the highest concentrations. This may be due to the different properties and surface reactivity of their surfaces. The toxicity of silane has been well-reviewed by Iler *et al.*²⁷. Addition of -NH₂ groups (Fig. 6) denote less accessible sites for biomolecules to attach in comparison to the uncoated SPIONs. The reduced toxicity of the Fe₃O₄ - APTS+PEG nanoparticles may be attributed to the high solubility of PEG in the cell membranes^{28,38}. However, there were still toxic effects on the soluble factors present in these nanoparticles, including detergents and monomers from the preparation procedure or the breakdown of products during incubation.

Surface functionalization of Fe₃O₄ - APTS nanoparticles

The peaks that appeared in (Fig.6) provide evidence that -COOH groups were attached to the surface through a reaction of -NH₂ and succinic anhydride at a transmittance of 119%^{29,39,40}. As the amine-terminated surface was converted to the aldehyde group, the characteristic band for HC=O vibration appeared at 1711 cm⁻¹ and CH₂-CHO at 1414 cm⁻¹, and CHO at 1374 cm⁻¹ indicating that the aldehyde group had been introduced to the SPION surfaces. The findings illustrated in (Fig. 6) indicated that the size of Fe₃O₄ - APTS+PEG was the largest, possibly either due to the high molecular weight of the polymer or due to the agglomerate of these particles.

Conclusions

Multifunctional magnetite nanoparticles have been successfully prepared by a co-precipitation method. By surface modification with APTS and subsequent functionalization with glutaraldehyde and succinic anhydride, these nanoparticles should have a high active binding to PyMSP1₁₉ malaria protein molecules (which is currently under study). XRD patterns indicated the high purity of the synthesized SPIONs, FTIR spectra confirmed that silane layer had been coated on the surface of Fe₃O₄. The SPIONs were superparamagnetic and were stable in aqueous phase at room temperature. VSM displayed relatively high magnetization (67 emu/g) at 15Koe of the iron oxide na-

noparticles. TEM images of bare and silane-coated nanoparticles were taken to investigate the size, shape and uniformity of the particles. The bare particles had a mean size of around 20 nm with relatively slim size distribution which also confirmed by Scanning Electron Micrograph (SEM). The fabricated nanoparticles were non-toxic which indicated by MTT assay. The particles can potentially be used as a platform to conjugate with other proteins including those targeting specific parasites. With the advantage of narrow size properties, relatively low toxicity, and ease of coupling with other biomolecules, we envision that these nanoparticles could be used as particulate vaccine in biomedical application.

Bibliographic references

- Halavaara J, Tervahartiala P, Isoniemi H, Höckerstedt K. Efficacy of sequential use of superparamagnetic iron oxide and gadolinium in liver MR imaging. *Acta radiologica*. 2002 Mar;43(2):180-5.
- Liberti PA, Rao CG, Terstappen LW. Optimization of ferrofluids and protocols for the enrichment of breast tumor cells in blood. *Journal of magnetism and magnetic materials*. 2001 1 January;225(1-2):301-7.
- Lübbe AS, Alexiou C, Bergemann C. Clinical applications of magnetic drug targeting. *Journal of Surgical Research*. 2001 Feb 1;95(2):200-6.
- Dormann JL, Fiorani D, Tronc E. Advances in chemical physics. Vol. XCVII, Eds. I. Prigogine y Stuart A. Rice, John Wiley and Sons. 1997.
- Tartaj P, Morales MP, Gonzalez-Carreño T, Veintemillas-Verdaguer S, Serna CJ. Advances in magnetic nanoparticles for biotechnology applications. *Journal of Magnetism and Magnetic Materials*. 2005 Apr 1;290:28-34.
- Li D, Teoh WY, Gooding JJ, Selomulya C, Amal R. Functionalization strategies for protease immobilization on magnetic nanoparticles. *Advanced Functional Materials*. 2010 9 June;20(11):1767-77.
- Cannon WR, Danforth SC, Flint JH, Haggerty JS, Marra RA. Sinterable Ceramic Powders from Laser-Driven Reactions: I, Process Description and Modeling. *Journal of the American Ceramic Society*. 1982 Jul;65(7):324-30.
- He R, You X, Shao J, Gao F, Pan B, Cui D. Core/shell fluorescent magnetic silica-coated composite nanoparticles for bioconjugation. *Nanotechnology*. 2007 6 July;18(31):315601.
- Rasband WS. US National Institute of Health. <http://rsb.info.nih.gov/ij>. 2006.
- Gupta AK, Wells S. Surface-modified superparamagnetic nanoparticles for drug delivery: preparation, characterization, and cytotoxicity studies. *IEEE transactions on nanobioscience*. 2004 Mar 15;3(1):66-73.
- Liu X, Ma Z, Xing J, Liu H. Preparation and characterization of amino-silane modified superparamagnetic silica nanospheres. *Journal of Magnetism and magnetic Materials*. 2004 Mar 1;270(1-2):1-6.
- Liu X, Xing J, Guan Y, Shan G, Liu H. Synthesis of amino-silane modified superparamagnetic silica supports and their use for protein immobilization. *Colloids and Surfaces A: Physicochemical and Engineering Aspects*. 2004 4 May;238(1-3):127-31.
- Sun J, Zhou S, Hou P, Yang Y, Weng J, Li X, Li M. Synthesis and characterization of biocompatible Fe₃O₄ nanoparticles. *Journal of biomedical materials research Part A*. 2007 Feb;80(2):333-41.
- Zaitsev VS, Filimonov DS, Presnyakov IA, Gambino RJ, Chu B. Physical and chemical properties of magnetite and magnetite-polymer nanoparticles and their colloidal dispersions. *Journal of Colloid and Interface Science*. 1999 Apr 1;212(1):49-57.
- Harris LA, Goff JD, Carmichael AY, Riffle JS, Harburn JJ, St. Pierre TG, Saunders M. Magnetite nanoparticle dispersions stabilized with triblock copolymers. *Chemistry of Materials*. 2003 25 March;15(6):1367-77.
- Saravanan P, Alam S, Mathur GN. Comparative study on the synthesis of γ-Fe₂O₃ and Fe₃O₄ nanocrystals using high-temperature solution-phase technique. *Journal of materials science letters*. 2003 Sep;22(18):1283-5.

18. Kim DK, Zhang Y, Voit W, Rao KV, Muhammed M. Synthesis and characterization of surfactant-coated superparamagnetic monodispersed iron oxide nanoparticles. *Journal of magnetism and Magnetic Materials*. 2001 1 January;225(1-2):30-6.
19. Montagne F, Mondain-Monval O, Pichot C, Mozzanega H, Elaissari A. Preparation and characterization of narrow sized (o/w) magnetic emulsion. *Journal of magnetism and magnetic materials*. 2002 Sep 1;250:302-12.
20. Cornell RM, Schwertmann U. *The iron oxides: structure, properties, reactions, occurrences and uses*. John Wiley & Sons; 2003 17 October.
21. Yamaoka T, Tabata Y, Ikada Y. Distribution and tissue uptake of poly (ethylene glycol) with different molecular weights after intravenous administration to mice. *Journal of pharmaceutical sciences*. 1994 1 April;83(4):601-6.
22. Weissleder R, Bogdanov A, Neuwelt EA, Papisov M. Long-circulating iron oxides for MR imaging. *Advanced Drug Delivery Reviews*. 1995 Sep 1;16(2-3):321-34.
23. Karlsson HL, Cronholm P, Gustafsson J, Moller L. Copper oxide nanoparticles are highly toxic: a comparison between metal oxide nanoparticles and carbon nanotubes. *Chemical research in toxicology*. 2008 Sep 15;21(9):1726-32.
24. Lacava ZG, Azevedo RB, Martins EV, Lacava LM, Freitas ML, Garcia VA, Rebula CA, Lemos AP, Sousa MH, Tourinho FA, Da Silva MF. Biological effects of magnetic fluids: toxicity studies. *Journal of magnetism and magnetic materials*. 1999 Jul 1;201(1-3):431-4.
25. Häfeli UD, Pauer GJ. In vitro and in vivo toxicity of magnetic microspheres. *Journal of magnetism and magnetic materials*. 1999 Apr 1;194(1-3):76-82.
26. Iler KR. *The chemistry of silica. Solubility, polymerization, colloid and surface properties and biochemistry of silica*. Wiley, New York. 1979: 89.
27. Jarrell BE, Williams SK, Stokes G, Hubbard FA, Carabasi RA, Koolpe E, Greener D, Pratt K, Moritz MJ, Radomski J. Use of freshly isolated capillary endothelial cells for the immediate establishment of a monolayer on a vascular graft at surgery. *Surgery*. 1986 1 August;100(2):392-9.
28. Liu C, Wu X, Klemmer T, Shukla N, Weller D, Roy AG, Tanase M, Laughlin D. Reduction of sintering during annealing of FePt nanoparticles coated with iron oxide. *Chemistry of materials*. 2005 8 February;17(3):620-5.
29. Feng B, Hong RY, Wang LS, Guo L, Li HZ, Ding J, Zheng Y, Wei DG. Synthesis of Fe₃O₄/APTES/PEG diacid functionalized magnetic nanoparticles for MR imaging. *Colloids and Surfaces A: Physicochemical and Engineering Aspects*. 2008 Oct 1;328(1-3):52-9.
30. Ajinkya N, Yu X, Kaithal P, Luo H, Somani P, Ramakrishna S. Magnetic Iron Oxide Nanoparticle (IONP) Synthesis to Applications: Present and Future. *Materials*. 2020 Jan;13(20):4644.
31. Cheah P, Cowan T, Zhang R, Fatemi-Ardekani A, Liu Y, Zheng J, Han F, Li Y, Cao D, Zhao Y. Continuous growth phenomenon for direct synthesis of monodisperse water-soluble iron oxide nanoparticles with extraordinarily high relaxivity. *Nanoscale*. 2020;12(16):9272-83.
32. Velázquez-Herrera FD, Fetter G. Hydrotalcites with heterogeneous anion distributions: a first approach to producing new materials to be used as vehicles for the successive delivery of compounds. *Clay Minerals*. 2020 Mar;55(1):31-9.
33. Yong KW, Yuen D, Chen MZ, Porter CJ, Johnston AP. Pointing in the right direction: controlling the orientation of proteins on nanoparticles improves targeting efficiency. *Nano letters*. 2019 Feb 18;19(3):1827-31.
34. Li X, Yang Y, Yang F, Wang F, Li H, Tian H, Wang G. Chitosan hydrogel loaded with recombinant protein containing epitope C from HSP90 of *Candida albicans* induces protective immune responses against systemic candidiasis. *International Journal of Biological Macromolecules*. 2021 Mar 15;173:327-40.
35. Nkurikiyimfura I, Wang Y, Safari B, Nshingabigwi E. Temperature-dependent magnetic properties of magnetite nanoparticles synthesized via coprecipitation method. *Journal of Alloys and Compounds*. 2020 15 December;846:156344.
36. Mostafaei M, Hosseini SN, Khatami M, Javidanbardan A, Sepahy AA, Asadi E. Isolation of recombinant Hepatitis B surface antigen with antibody-conjugated superparamagnetic Fe₃O₄/SiO₂ core-shell nanoparticles. *Protein expression and purification*. 2018 1 May;145:1-6.
37. Yew YP, Shameli K, Miyake M, Khairudin NB, Mohamad SE, Naiki T, Lee KX. Green biosynthesis of superparamagnetic magnetite Fe₃O₄ nanoparticles and biomedical applications in targeted anticancer drug delivery system: A review. *Arabian Journal of Chemistry*. 2020 1 January;13(1):2287-308.
38. Sharma A, Jyoti K, Bansal V, Jain UK, Bhushan B, Madan J. Soluble telmisartan bearing poly (ethylene glycol) conjugated chitosan nanoparticles augmented drug delivery, cytotoxicity, apoptosis and cellular uptake in human cervical cancer cells. *Materials Science and Engineering: C*. 2017 1 March;72:69-76.
39. Shagholani H, Ghoreishi SM, Sharifi SH. Conversion of amine groups on chitosan-coated SPIONs into carbocyclic acid and investigation of its interaction with BSA in drug delivery systems. *Journal of Drug Delivery Science and Technology*. 2018 1 June;45:373-7.
40. Ikonen T, Kalidas N, Lahtinen K, Isoniemi T, Toppari JJ, Vázquez E, Herrero-Chamorro MA, Fierro JL, Kallio T, Lehto VP. Conjugation with carbon nanotubes improves the performance of mesoporous silicon as Li-ion battery anode. *Scientific reports*. 2020 27 March;10(1):1-8.
41. Filipczak P, Borkowski M, Chudobinski P, Bres S, Matusiak M, Nowaczyk G, Kozanecki M. Sodium citrate stabilized Ag NPs under thermal treatment, electron-beam and laser irradiations. *Radiation Physics and Chemistry*. 2020 1 April;169:107948.
42. Albukhaty S, Naderi-Manesh H, Tiraihi T, Sakhi Jabir M. Poly-L-lysine-coated superparamagnetic nanoparticles: a novel method for the transfection of pro-BDNF into neural stem cells. *Artificial cells, nanomedicine, and biotechnology*. 2018 Nov 12;46(sup3):S125-32.
43. Albukhaty S, Al-Musawi S, Abdul Mahdi S, Sulaiman GM, Alwahibi MS, Dewir YH, Soliman DA, Rizwana H. Investigation of Dextran-Coated Superparamagnetic Nanoparticles for Targeted Vinblastine Controlled Release, Delivery, Apoptosis Induction, and Gene Expression in Pancreatic Cancer Cells. *Molecules*. 2020 Jan;25(20):4721.
44. Banoon SR, Ghasemian A. The Characters of Graphene Oxide Nanoparticles and Doxorubicin Against HCT-116 Colorectal Cancer Cells In Vitro. *Journal of Gastrointestinal Cancer*. 2021 Mar 19:1-5.

Received: 10 April 2021

Accepted: 15 July 2021